

The synthesis and application of a colour-switch β -arylethenesulfonyl fluoride fluorescent probe in the detection of serum albumin

Marie-Claire Giel^A, Tze Cin Owyong^{A,B} and Yuning Hong^{A,*} 

For full list of author affiliations and declarations see end of paper

***Correspondence to:**

Yuning Hong
Department of Biochemistry and Chemistry, La Trobe Institute for Molecular Science, La Trobe University, Melbourne, Vic. 3086, Australia
Email: y.hong@latrobe.edu.au

[§]Yuning Hong is the recipient of the 2022 Le Fèvre Medal from Australian Academy of Science.

Handling Editor:

Curt Wenstrup

Received: 27 July 2022

Accepted: 26 September 2022

Published: 22 November 2022

Cite this:

Giel M-C et al. (2022)
Australian Journal of Chemistry
75(11), 877–883. doi:10.1071/CH22165

© 2022 The Author(s) (or their employer(s)). Published by CSIRO Publishing.

This is an open access article distributed under the Creative Commons Attribution-NonCommercial-NoDerivatives 4.0 International License ([CC BY-NC-ND](https://creativecommons.org/licenses/by-nc-nd/4.0/))

OPEN ACCESS

ABSTRACT

Proteins play a pivotal role in regulating important physiological processes and serve as important biomarkers for many diseases. Herein, we present a new strategy for bovine serum albumin (BSA) detection using a novel colour-switch fluorescent probe CPV-ESF ((E)-2-(4-((Z)-1-cyano-2-(4-(diethylamino)phenyl)vinyl)phenyl)ethene-1-sulfonyl fluoride). CPV-ESF reacts with nucleophilic amino acids of BSA via 1,4-Michael addition click chemistry to create a covalently linked CPV-ESF:BSA complex, which can be easily detected by a fluorescence colour-switch response. The sensing mechanism, sensitivity and selectivity of CPV-ESF for BSA detection as well as its application for cell imaging have been investigated.

Keywords: 1,4-Michael addition chemistry, aggregation-induced emission, BSA, click chemistry, fluorescence probe, protein detection.

Protein detection is of fundamental importance in biological research and medical diagnosis.^[1] Of all the proteins, serum albumin is the most abundant in blood plasma (55–60%) and has many physiological functions such as functioning as a transporter for carrying, distributing and delivering different exogenous or endogenous ions, fatty acids and small molecules, such as pharmaceuticals, in the body.^[2] Many diseases alter the distribution of albumin between the intravascular and extravascular compartments; therefore, detecting human serum albumin (HSA) levels in biological fluids is of clinical importance for the diagnosis of many diseases, such as cancer, diabetes, liver disease, inflammation, rheumatic disease and cardiovascular diseases. For example, urinary albumin is deemed an important clinical indicator of chronic kidney disease (CKD).^[3,4] Bovine serum albumin (BSA) is composed of 583 amino acid residues and its secondary structure is the most analogous to HSA as they share 76% amino acid sequence homology, and it has therefore been widely investigated as a substitute for HSA in different fields owing to its availability and lower cost.^[5,6] Furthermore, owing to its stability and non-interference, BSA has been used in biochemical applications as a protein concentration standard, enzyme stabilizer, and in ion and protease detection, etc.^[7] Owing to its wide range of applications, the determination of BSA concentration has received considerable research interest. Conventional approaches for the detection of BSA include radioimmunoassay and enzyme-linked immunosorbent assay.^[8,9] However, these methods involve expensive reagents and complex preparation, limiting the application of these techniques. Therefore, there is a high demand for rapid, simple, convenient methodologies for protein detection in biological samples.

Fluorescence is an indispensable technique for visualizing proteins, tracking physiological and pathological processes and diagnosing diseases in complex biological systems.^[10] Small molecule ‘switchable’ fluorescent probes, which induce changes in the fluorescence properties (intensity and/or wavelength) upon interaction with the target analyte, are particularly useful for this purpose because they allow simple and rapid detection.^[11–13] The most prevalent probes for the detection of proteins are fluorogenic substrates that allow the monitoring of hydrolases,^[14,15] such as glycosidases

and proteases, by either turn-on fluorescence or fluorescence resonance energy transfer (FRET).^[16] However, the design of fluorescence probes for non-enzymatic proteins remains more challenging and they often rely on non-covalent interactions that can be affected by reaction medium, ionic strength, surface morphology and protein foldedness, thus having a low reliability.^[17,18] Recently, peptide-based molecular beacons have been reported for proteins that bind specific short peptide sequences.^[19] However, the limitation of the beacon system is that it can only be applied to polypeptide-binding protein receptors. Additionally, many small molecule fluorescent probes suffer from the aggregation-caused quenching (ACQ) effect.^[20] The fluorescence intensity decreases dramatically when the fluorescent molecules are used at high concentration or in the solid state. For example, even a dilute solution (10 μM) of *N,N*-dicyclohexyl-1,7-dibromo-3,4,9,10-perylenetetracarboxylic diimide (DDPD) in THF is highly luminescent but its emission weakens when water is added to the THF, owing to the immiscibility of DDPD with water, which increases the local luminophore concentration and causes the DDPD molecules to aggregate, leading to an ACQ effect.^[21] Like DDPD, pyrene is also an ACQ luminophore. In the low concentration region ($c < 0.1 \mu\text{M}$), it is highly emissive at 390 nm. However, when its concentration is increased to 0.1 mM, its emission becomes weaker and further increasing the concentration leads to a corresponding decrease in its emission intensity until, at the concentration of 0.1 M, the peak at 390 nm disappears owing to the concentration-quenching effect.^[21]

While the ACQ effect can be beneficial,^[22] it can also compromise the performance and application of organic dyes as biosensors in many scenarios, as the biosensors can only be used in dilute solutions, which limits the sensitivity and signal-to-background ratio.^[23,24] The use of ACQ dyes in imaging processes is also limited as they are used in very dilute solutions and such small numbers of dye molecules can be quickly photobleached when a harsh laser beam is used as the excitation light source. The photostability cannot be improved by using higher fluorophore concentration owing to the accompanying concentration-quenching effect.^[25] Furthermore, the ACQ effect is often favourable for developing fluorescent turn-off biosensors, rather than their turn-on counterparts; fluorescent turn-on sensors have many advantages compared with fluorescent turn-off sensors, such as a lower detection limit, higher signal-to-background ratio and higher sensitivity.^[26] The development of aggregation-induced emission luminogens (AIEgens) has provided an excellent class of fluorescent scaffolds for protein detection. The concept of aggregation-induced emission (AIE) refers to a unique phenomenon where some fluorogens are non-emissive or weakly emissive in dilute solutions but become highly luminescent when the molecules are aggregated in concentrated solutions. The emergence of luminogens with AIE characteristics addresses the deficiencies of ACQ fluorophores.^[21]

β -Arylethanesulfonyl fluorides have excellent biocompatibility as clickable functionalities and have been widely applied across several diverse areas of chemistry.^[27,28] However, despite their versatile reactivity and potential, the use of β -arylethanesulfonyl fluorides in fluorescence technologies remains underexploited. Recently, we reported the first β -arylethanesulfonyl fluoride fluorogenic probe, which was successfully applied for the detection of trypsin.^[29] Herein, we demonstrate the potential of a new colour-switch β -arylethanesulfonyl fluoride fluorescent probe (*E*)-2-(4-((*Z*)-1-cyano-2-(4-(diethylamino)phenyl)vinyl)phenyl)ethene-1-sulfonyl fluoride (CPV-ESF) with AIE properties that could be widely used for the detection of proteins. In contrast to our previous β -arylethanesulfonyl fluoride probe, which was non-fluorescent when molecularly dissolved in aqueous solution, CPV-ESF remains strongly emissive and therefore is able to function as a colour-switch fluorescent probe. Equipped with a highly electrophilic vinyl sulfonyl fluoride moiety, CPV-ESF can conjugate to proteins such as BSA via a 1,4-Michael addition reaction with nucleophilic amino acid side chains (cysteine and lysine), leading to a change in π -conjugation, which can be easily detected by UV-vis or fluorescence spectroscopy (Fig. 1).^[30]

CPV-ESF was synthesized in a simple two-step procedure (Supplementary Scheme S1) and was characterized by ¹H, ¹³C and ¹⁹F NMR spectroscopy and high-resolution mass spectrometry. The synthesis began with a Knoevenagel condensation between 4-(diethylamino)benzaldehyde and 2-(4-iodophenyl)acetonitrile to give the donor-acceptor (D-A) core,^[31] followed by a palladium-catalyzed fluorosulfonyl-vinylation to introduce the vinyl sulfonyl fluoride functionality ready for covalent bond formation. CPV-ESF displays strong fluorescence on aggregation or in the solid state, features characteristic of typical AIE active molecules, inspiring us to investigate the AIE properties further. CPV-ESF possesses an absorption and an emission maximum at 455 and 625 nm respectively in DMSO solution, with a large Stoke shift of 170 nm observed (Fig. 2a). We then used mixed solvent systems (DMSO/toluene (Fig. 2b), DMSO/H₂O (Fig. 2c), DMSO/CHCl₃ (Supplementary Fig. S1)) to evaluate the AIE properties of CPV-ESF. Fluorescence spectra of CPV-ESF in DMSO with increasing content of water, a

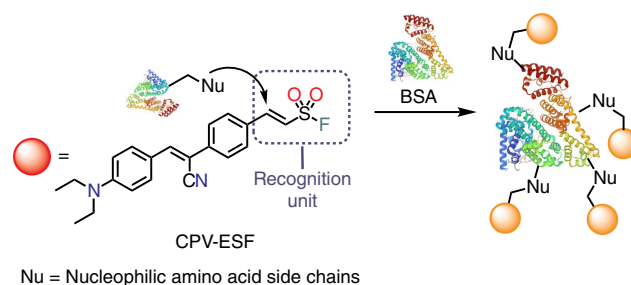


Fig. 1. Design rationale of CPV-ESF and the mechanism of conjugation of BSA.

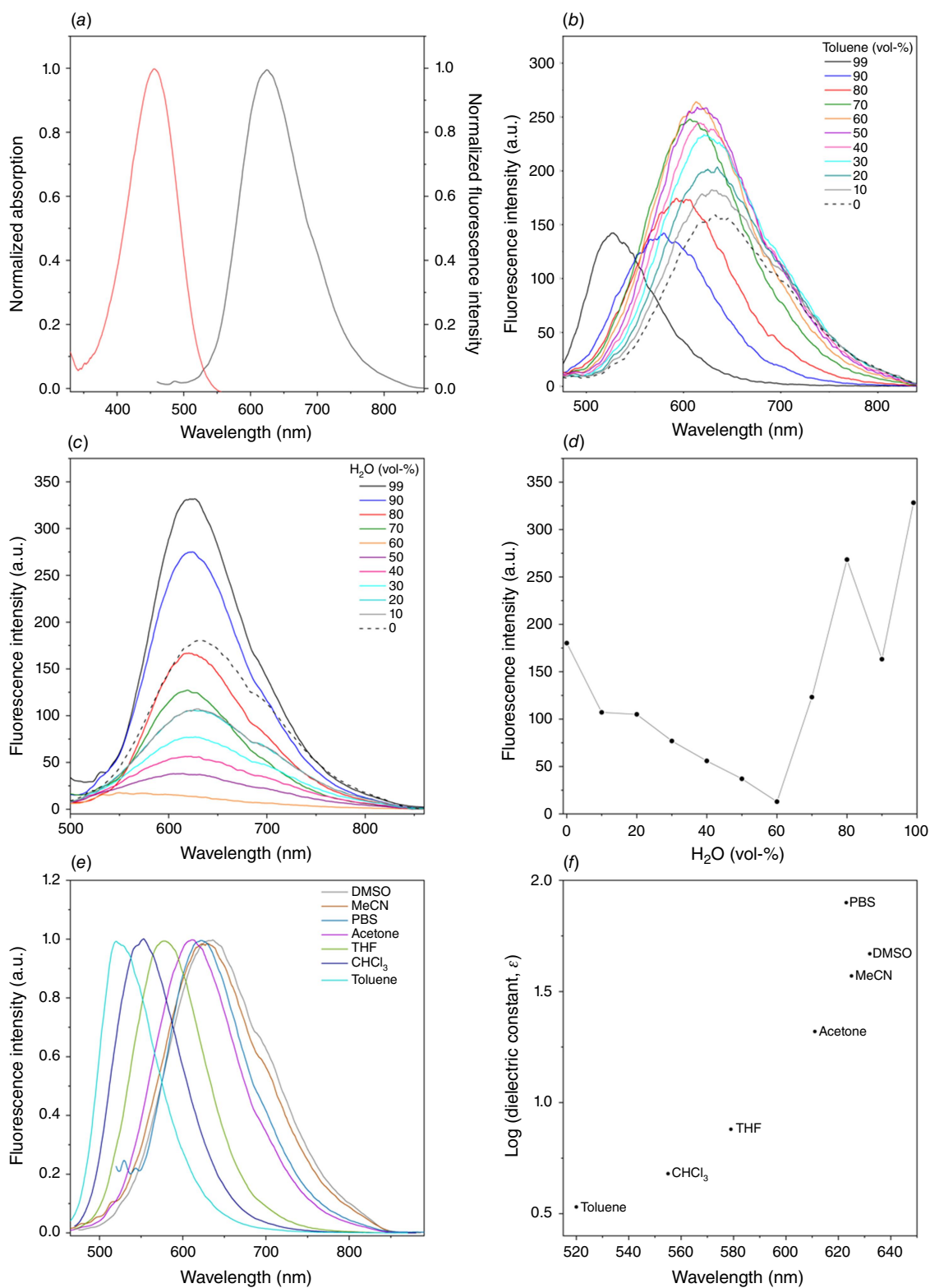


Fig. 2. (Caption on next page)

Fig. 2. Photophysical characterization of CPV-ESF: (a) Normalized UV/vis absorbance of CPV-ESF (red) in DMSO and emission spectrum (black) in 99% H₂O. (b) Fluorescence emission spectra of CPV-ESF in toluene/DMSO mixtures, with increasing fraction of toluene from 0 to 99%. (c) Fluorescence emission spectra of CPV-ESF in DMSO/H₂O mixtures, with increasing fraction of H₂O from 0 to 99%. (d) Plot of fluorescence intensity of CPV-ESF at 620 nm in DMSO/H₂O mixtures, with increasing fraction of H₂O from 0 to 99%. (e) Normalized fluorescence spectra of CPV-ESF in solvents with different polarity. (f) Correlation of emission maximum of CPV-ESF in solvents with different polarity vs dielectric constant (ϵ) of solvent in logarithm; 50 μ M dye concentration and 440 nm excitation wavelength were used for all measurements.

poor solvent for CPV-ESF, are shown in Fig. 2c, d. At a low water fraction, affected by the electron donor–acceptor (D-A) structure, the emission of CPV-ESF became suppressed in polar solvent owing to the twisted intramolecular charge transfer (TICT) effect.^[32] However, at higher water fractions, fluorescence intensity enhancement was observed, demonstrating the AIE nature of the molecule. Meanwhile, when toluene was used as the poor solvent with DMSO, an increase in fluorescence intensity was observed up to 60%. However, increasing the content of toluene beyond this, the fluorescence emission of CPV-ESF decreased with a blue shift, which we attribute to the low polarity of toluene and the poor solubility of CPV-ESF in toluene resulting in its precipitation (Fig. 2b). As shown in Supplementary Fig. S1, when CHCl₃ was used as a poor solvent, no significant fluorescence intensity change was observed with increasing CHCl₃ fraction until 90% CHCl₃, where a decrease in fluorescence emission intensity was seen again, with a blue shift possibly due to the poor solubility in CPV-ESF. The observed spectral shift in CPV-ESF when solvents of varying polarity were used led us to investigate the solvatochromic nature of CPV-ESF. As shown in Fig. 2e, only a minimal change in spectral shift of CPV-ESF was observed in polar solvents such as phosphate buffer saline (PBS) buffer, DMSO and acetonitrile. However, for less polar solvents, the emission spectra displayed a blue shift with decreasing solvent polarity. Overall, the emission peak shifted from 520 nm in non-polar toluene to 632 nm in PBS solution. When comparing the emission maximum and the logarithm of the dielectric constant of the solvents, we found a large change in the CPV-ESF emission maximum in less polar solvents (toluene, CHCl₃, THF) relative to polar solvents (acetone, MeCN, DMSO, PBS buffer) (Fig. 2f).

Following the photophysical characterization of CPV-ESF, we investigated the ability of CPV-ESF to detect BSA. In our initial test, we incubated BSA (10 μ M) with CPV-ESF (100 μ M) at 37°C in NaHCO₃ buffer for 1 h. As shown in Supplementary Fig. S2, a blue-shifted spectral profile was observed in comparison with CPV-ESF itself. The spectral differences of CPV-ESF following incubation with BSA can be rationalized by the extension of the π -conjugate of the vinyl group and the contribution of the electron-withdrawing sulfonyl fluoride of CPV-ESF, which was removed following conjugation to BSA; thus, a hypsochromic shift was observed, enabling the detection of BSA. We initially performed the experiments in NaHCO₃ buffer at pH 9 assuming a basic environment was needed to facilitate the

1,4-Michael addition reaction; however, conjugation between CPV-ESF and BSA worked similarly well at pH 7 in PBS buffer (Supplementary Fig. S2). Next, we performed a fluorescence titration experiment to further investigate the effect of BSA on its fluorescence intensity. As indicated in Fig. 3a, the fluorescence intensity of CPV-ESF (100 μ M) originally peaked at 620 nm and then shifted to 530 nm in the presence of BSA. Intriguingly, the fluorescence intensity ratio at 530 and 620 nm (I_{530}/I_{620}) increased with increasing BSA concentration in an inversely exponential manner (Fig. 3b). At lower BSA concentration (up to 2.0 μ M), a linear relationship between I_{530}/I_{620} and the BSA concentration was found, from which we obtained the limit of detection (LOD) with the equation $\text{LOD} = 3\sigma/K$, where σ , the standard deviation, denotes the standard deviation for three blank readings and K is the slope of the fitted line. The LOD of the CPV-ESF for BSA was calculated to be 0.11 μ M (or 7.26 mg/L), which would be suitable for applications like urinary albumin detection. The specificity of CPV-ESF for BSA detection was also examined using a selection of proteins and common biomolecules, including glutathione (GSH) and cysteine, to which CPV-ESF could potentially bind. As shown in Fig. 3c, d, following incubation for 1 h, only BSA induced a clear hypsochromic shift in comparison with CPV-ESF and gave the strongest fluorescence intensity ratio at 530 and 620 nm.

Finally, preliminary investigations into our proposed sensing mechanism were performed using the surrogate compound S1 where the double bond had already reacted, therefore blocking the reactive site (Fig. 3e, f). As previously shown, incubation of CPV-ESF with BSA results in a blue-shifted spectral profile that we propose is due the change in π -conjugation. However, in compound S1, the double bond recognition site has already reacted and therefore it was proposed that no change in fluorescence would occur. As shown in Fig. 3e, no change in fluorescence was observed following incubation of compound S1 with BSA for 1 h at 37°C in contrast to the spectral shift observed with CPV-ESF and BSA. This observation is supported by density functional theory (DFT) calculations that showed CPV-ESF had an electron donor–acceptor type structure, with the HOMO localized on the electron-donating diethylamino group and LUMO localized on the electron-withdrawing β -arylethanesulfonyl fluoride group. On reaction with the model system of morpholine, we observed similar localization of the HOMO on the electron-donating diethylamino group, while the LUMO was more localized on the electron-withdrawing cyano

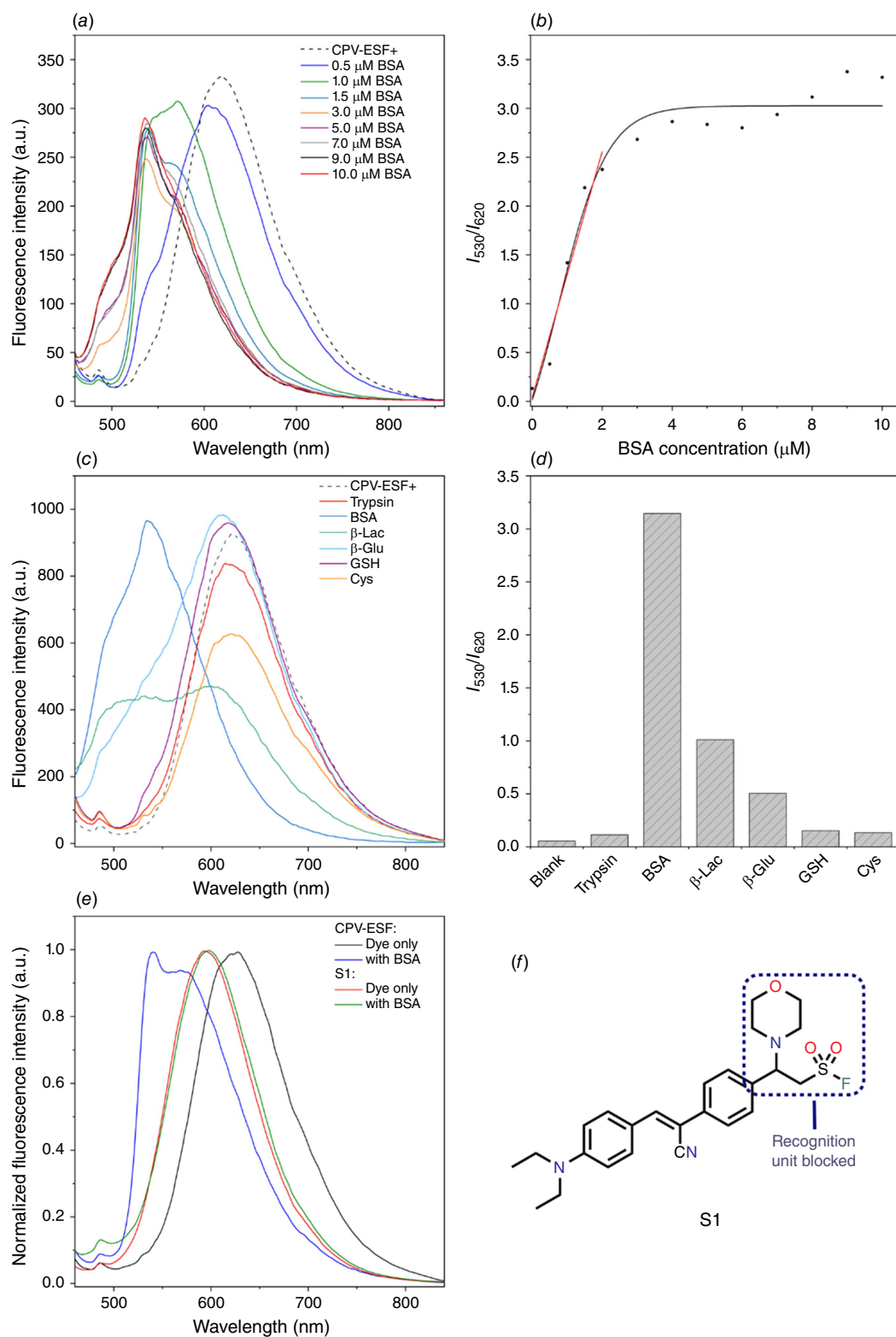


Fig. 3. (Caption on next page)

Fig. 3. Formation of CPV-ESF:BSA complex. (a) Fluorescence emission spectra of CPV-ESF (100 μM) with varying concentration of BSA (1–10 μM) in PBS buffer solution. (b) Plot of fluorescence intensity ratio (I_{530}/I_{620}) vs BSA concentration for determination of the LOD. (c) Fluorescence response of CPV-ESF (100 μM) after addition of different proteins and biomolecules (10 μM) in PBS buffer solution. (d) Fluorescence intensity ratio (I_{530}/I_{620}) variation of CPV-ESF (100 μM) after addition of different proteins and biomolecules (10 μM) at 530 nm. (e) Fluorescence emission spectra demonstrating the difference in reactivity of CPV-ESF and SI towards BSA in PBS buffer solution. (f) Surrogate compound, SI. A 440-nm excitation wavelength was used for all measurements. GSH, glutathione.

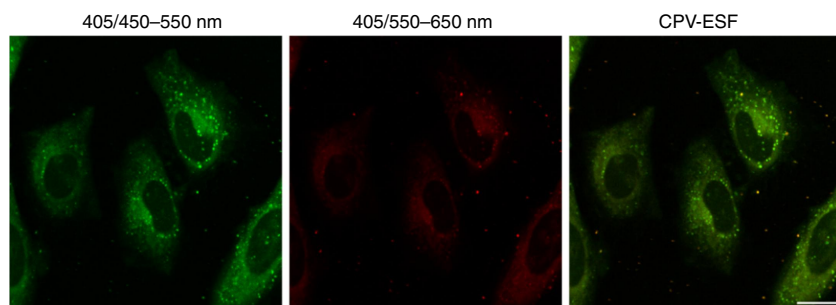


Fig. 4. Confocal images of CPV-ESF-stained HeLa cells. HeLa cells were stained with 10 μM CPV-ESF for 0.5 h before fixation. Scale bar, 20 μm .

group. We attribute the larger energy gap observed in the reacted form of CPV-ESF (2.92–3.33 eV) to the loss of conjugation (Supplementary Fig. S3). Furthermore, in our previous work on β -arylethanesulfonyl fluoride fluorogenic probes, we demonstrated BSA covalently modified the probe using sodium dodecyl-sulfate polyacrylamide gel electrophoresis (SDS-PAGE); as CPV-ESF has the same recognition moiety, they are likely to have the same sensing mechanism. Cumulatively, this suggests that the sensing mechanism is a covalent reaction between the electrophilic double bond of CPV-ESF and nucleophilic residues of BSA, which offers additional advantages over previous methods. Lastly, we incubated the pre-formed CPV-ESF:BSA complex (100:10 μM) with trypsin at 37°C for 1 h. A fluorescence turn-off effect was then observed (Supplementary Fig. S4), suggesting the digestion of BSA by the protease trypsin and highlighting the importance of the AIE effect in the detection process of BSA.

We observed good uptake of CPV-ESF in cells when doing confocal laser scanning microscopy experiments (Fig. 4). CPV-ESF uptake was further validated by use of Z-stack image acquisition showing dye penetration in both cytoplasm and nucleus. These results highlight the promise of CPV-ESF as a chemical tag for future experiments in biological systems.

In summary, we synthesized and applied the novel fluorescent probe (*E*)-2-(4-((*Z*)-1-cyano-2-(4-(diethylamino)phenyl)vinyl)phenyl)ethene-1-sulfonyl fluoride (CPV-ESF) for a straightforward method for BSA detection. Compared with previous BSA detection methods, the CPV-ESF:BSA sensing system is simple to prepare and its formation is easily detected using UV-vis or fluorescence spectroscopy owing to change in π -conjugation. Furthermore, preliminary investigations suggest the sensing mechanism to be via a covalent reaction between CPV-ESF and BSA and the AIE characteristics of CPV-ESF, offering several advantages over

previous methods. Collectively, this proof-of-concept study demonstrates the potential of CPV-ESF as a simple fluorescence protocol for the detection of BSA.

Supplementary material

Supplementary material is available [online](#).

References

- [1] Lv Z, Liu J, Bai W, Yang S, Chen A. A simple and sensitive label-free fluorescent approach for protein detection based on a perylene probe and aptamer. *Biosens Bioelectron* 2015; 64: 530–534. doi:10.1016/j.bios.2014.09.095
- [2] Jahanban-Esfahlan A, Ostadrahimi A, Jahanban-Esfahlan R, Roufegarinejad L, Tabibiazar M, Amarowicz R. Recent developments in the detection of bovine serum albumin. *Int J Biol Macromol* 2019; 138: 602–617. doi:10.1016/j.ijbiomac.2019.07.096
- [3] Hu Q, Yao B, Owyong TC, Prashanth S, Wang C, Zhang X, Wong WWH, Tang Y, Hong Y. Detection of urinary albumin using a ‘turn-on’ fluorescent probe with aggregation-induced emission characteristics. *Chem Asian J* 2021; 16: 1245–1252. doi:10.1002/asia.202100180
- [4] Yao B, Giel M-C, Hong Y. Detection of kidney disease biomarkers based on fluorescence technology. *Mater Chem Front* 2021; 5: 2124–2142. doi:10.1039/D0QM01009J
- [5] Babu E, Muthu Mareeswaran P, Singaravadevel S, Bhuvaneshwari J, Rajagopal S. A selective, long-lived deep-red emissive ruthenium(II) polypyridine complexes for the detection of BSA. *Spectrochim Acta A Mol Biomol Spectrosc* 2014; 130: 553–560. doi:10.1016/j.saa.2014.04.060
- [6] MacManus-Spencer LA, Tse ML, Hebert PC, Bischel HN, Luthy RG. Binding of perfluorocarboxylates to serum albumin: a comparison of analytical methods. *Anal Chem* 2010; 82: 974–981. doi:10.1021/ac902238u
- [7] Zhang LL, Ma FF, Kuang YF, Cheng S, Long YF, Xiao QG. Highly sensitive detection of bovine serum albumin based on the aggregation of triangular silver nanoplates. *Spectrochim Acta A Mol Biomol Spectrosc* 2016; 154: 98–102. doi:10.1016/j.saa.2015.10.019
- [8] Zhao D, Zhang Q, Zhang Y, Liu Y, Pei Z, Yuan Z, Sang S. Sandwich-type surface stress biosensor based on self-assembled gold nanoparticles in PDMS film for BSA Detection. *ACS Biomater Sci Eng* 2019; 5: 6274–6280. doi:10.1021/acsbomaterials.9b01073

- [9] Lin T-Y, Hu C-H, Chou T-C. Determination of albumin concentration by MIP-QCM sensor. *Biosens Bioelectron* 2004; 20: 75–81. doi:10.1016/j.bios.2004.01.028
- [10] Wu M-Y, Leung J-K, Liu L, Kam C, Chan KYK, Li RA, Feng S, Chen S. A small-molecule AIE chromosome periphery probe for cytogenetic studies. *Angew Chem Int Ed* 2020; 59: 10327–10331. doi:10.1002/anie.201916718
- [11] Kobayashi H, Ogawa M, Alford R, Choyke PL, Urano Y. New strategies for fluorescent probe design in medical diagnostic imaging. *Chem Rev* 2010; 110: 2620–2640. doi:10.1021/cr900263j
- [12] Lavis LD, Raines RT. Bright ideas for chemical biology. *ACS Chem Biol* 2008; 3: 142–155. doi:10.1021/cb700248m
- [13] Li H, Kim H, Han J, Nguyen V-N, Peng X, Yoon J. Activity-based smart AIEgens for detection, bioimaging, and therapeutics: recent progress and outlook. *Aggregate* 2021; 2: 1–30. doi:10.1002/agt2.51
- [14] Kamiya M, Kobayashi H, Hama Y, Koyama Y, Bernardo M, Nagano T, Choyke PL, Urano Y. An enzymatically activated fluorescence probe for targeted tumor imaging. *J Am Chem Soc* 2007; 129: 3918–3929. doi:10.1021/ja067710a
- [15] Mei J, Tian H. Most recent advances on enzyme-activatable optical probes for bioimaging. *Aggregate* 2021; 2: 1–34. doi:10.1002/agt2.32
- [16] Pham W, Choi Y, Weissleder R, Tung C-H. Developing a peptide-based near-infrared molecular probe for protease sensing. *Bioconjugate Chem* 2004; 15: 1403–1407. doi:10.1021/bc049924s
- [17] Mizusawa K, Ishida Y, Takaoka Y, Miyagawa M, Tsukiji S, Hamachi I. Disassembly-driven turn-on fluorescent nanoprobe for selective protein detection. *J Am Chem Soc* 2010; 132: 7291–7293. doi:10.1021/ja101879g
- [18] Hong Y, Feng C, Yu Y, Liu J, Lam JWY, Luo KQ, Tang BZ. Quantitation, visualization, and monitoring of conformational transitions of human serum albumin by a tetraphenylethene derivative with aggregation-induced emission characteristics. *Anal Chem* 2010; 82: 7035–7043. doi:10.1021/ac1018028
- [19] Thurley S, Röglin L, Seitz O. Hairpin peptide beacon: dual-labeled PNA-peptide-hybrids for protein detection. *J Am Chem Soc* 2007; 129: 12693–12695. doi:10.1021/ja075487r
- [20] Borisov SM, Wolfbeis OS. Optical biosensors. *Chem Rev* 2008; 108: 423–461. doi:10.1021/cr068105t
- [21] Hong Y, Lam JWY, Tang BZ. Aggregation-induced emission. *Chem Soc Rev* 2011; 40: 5361–5388. doi:10.1039/c1cs15113d
- [22] Chen RF, Knutson JR. Mechanism of fluorescence concentration quenching of carboxyfluorescein in liposomes: energy transfer to non-fluorescent dimers. *Anal Biochem* 1988; 172: 61–77. doi:10.1016/0003-2697(88)90412-5
- [23] Kim HN, Lee MH, Kim HJ, Kim JS, Yoon J. A new trend in rhodamine-based chemosensors: application of spirolactam ring-opening to sensing ions. *Chem Soc Rev* 2008; 37: 1465–1472. doi:10.1039/b802497a
- [24] Fan L-J, Jones Jr WE. A highly selective and sensitive inorganic/organic hybrid polymer fluorescence ‘turn-on’ chemosensory system for iron cations. *J Am Chem Soc* 2006; 128: 6784–6785. doi:10.1021/ja0612697
- [25] Leung CWT, Hong Y, Chen S, Zhao E, Lam JWY, Tang BZ. A photostable AIE luminogen for specific mitochondrial imaging and tracking. *J Am Chem Soc* 2013; 135: 62–65. doi:10.1021/ja310324q
- [26] Mao L, Liu Y, Yang S, Li Y, Zhang X, Wei Y. Recent advances and progress of fluorescent bio-/chemosensors based on aggregation-induced emission molecules. *Dyes Pigm* 2019; 162: 611–623. doi:10.1016/j.dyepig.2018.10.045
- [27] Zha G-F, Wang S-M, Rakesh KP, Bukhari SNA, Manukumar HM, Vivek HK, Mallesha N, Qin H-L. Discovery of novel arylolethene-sulfonyl fluorides as potential candidates against methicillin-resistant of *Staphylococcus aureus* (MRSA) for overcoming multi-drug resistance of bacterial infections. *Eur J Med Chem* 2019; 162: 364–377. doi:10.1016/j.ejmech.2018.11.012
- [28] Brouwer AJ, Herrero Álvarez N, Ciaffoni A, van de Langemheen H, Liskamp RMJ. Proteasome inhibition by new dual warhead containing peptido vinyl sulfonyl fluorides. *Bioorg Med Chem* 2016; 24: 3429–3435. doi:10.1016/j.bmc.2016.05.042
- [29] Giel M-C, Zhang S, Hu Q, Ding D, Tang Y, Hong Y. Synthesis of a β -arylolethene-sulfonyl fluoride-functionalized AIEgen for activity-based urinary trypsin detection. *ACS Appl Bio Mater* 2022; 5: 4321–4326. doi:10.1021/acsabm.2c00513
- [30] Giel M-C, Hong Y. The application of click chemistry in the design of aggregation-induced emission luminogens for activity-based sensing. In: Gu X, Tang BZ, editors *Aggregation-Induced Emission: Applications in Biosensing, Bioimaging and Biomedicine*. Vol. 1. Berlin, Germany: De Gruyter; 2022. pp. 53–82. doi:10.1515/9783110672220-004
- [31] OwYong TC, Ding S, Wu N, Fellowes T, Chen S, White JM, Wong WWH, Hong Y. Optimising molecular rotors to AIE fluorophores for mitochondria uptake and retention. *Chem Commun* 2020; 56: 14853–14856. doi:10.1039/D0CC06411D
- [32] Sasaki S, Drummen GPC, Konishi G. Recent advances in twisted intramolecular charge transfer (TICT) fluorescence and related phenomena in materials chemistry. *J Mater Chem C* 2016; 4: 2731–2743. doi:10.1039/C5TC03933A

Data availability. Data are available on request.

Conflicts of interest. The authors declare no conflict of interest.

Declaration of funding. This work was supported by funding from the Australian Research Council (FT210100271) and Australia–China Science and Research Fund Joint Research Centre on Personal Health Technologies (ACSRF65777).

Acknowledgements. We thank LIMS Comprehensive Proteomics Platform for the access to mass spectrometry and NMR facilities.

Author contributions. The manuscript was written through contributions of all authors. All authors have given approval to the final version of the manuscript.

Author affiliations

^ADepartment of Biochemistry and Chemistry, La Trobe Institute for Molecular Science, La Trobe University, Melbourne, Vic. 3086, Australia.

^BSchool of Chemistry, The University of Melbourne, Parkville, Vic. 3010, Australia.